Contrast-enhanced voiding ultrasonography to detect intrarenal reflux in children: comparison with 99mTc-DMSA renal scans

ULTRA SONO GRAPHY

Saelin Oh[1], Ji Young Ha[2], Yeon Jin Cho[3]

[1]Department of Radiology, Korea University Anam Hospital, Seoul; [2]Department of Radiology, Gyeongsang National University Changwon Hospital, Changwon; [3]Department of Radiology, Seoul National University Hospital, Seoul, Korea

ORIGINAL ARTICLE

https://doi.org/10.14366/usg.21143
pISSN: 2288-5919 • eISSN: 2288-5943
Ultrasonography 2022;41:502-510

Purpose: This study evaluated the diagnostic performance of contrast-enhanced voiding ultrasonography (CeVUS) for detecting intrarenal reflux (IRR) and the correlation between CeVUS-detected IRR sites and photon defect sites in acute ^{99m}Tc-dimercaptosuccinic acid (DMSA) renal scans in pediatric patients.

Methods: Fifty-four kidneys from 27 patients (20 males and seven females; mean age, 5.6±4.1 months) who underwent CeVUS and acute DMSA renal scans for recurrent urinary tract infection (UTIs) or pyelonephritis were included. Pediatric experts compared the results of CeVUS with acute DMSA renal scans.

Results: Thirteen renal units (13/54, 24.1%) in 10 patients (nine males and one female; mean age, 6.3±3.7 months; age range, 0 to 13 months) showed vesicoureteral reflux and eight renal units (8/54, 14.8%) demonstrated IRR on CeVUS. Ten renal units in eight patients (six males and two females; mean age, 6.9±1.4 months; age range, 2 to 13 months) showed 19 photon defects on acute DMSA renal scans. Fifty-two renal units (96.3%) showed concordant results, and two renal units (3.7%) showed discordant results between CeVUS and acute DMSA renal scans. IRR accounted for 15/19 (78.9%) photon defects in eight renal units of seven patients using CeVUS. In a per-renal-unit analysis, the sensitivity, specificity, positive predictive value, negative predictive value, and accuracy of CeVUS were 80%, 100%, 100%, 95.7%, and 96.3%, respectively.

Conclusion: CeVUS showed good performance in detecting IRR, and the IRR sites detected by CeVUS closely correlated with photon defect sites in acute DMSA scans. CeVUS may play an important role in managing patients with recurrent UTIs or pyelonephritis with reduced radiation exposure.

Keywords: Contrast-enhanced voiding ultrasonography; Technetium Tc 99m dimercaptosuccinic acid; Vesicoureteral reflux; Intrarenal reflux; Ultrasonography

Key points: Intrarenal refluxsites detected by contrast-enhanced voiding ultrasonography (CeVUS) and sites of photon defects in acute ^{99m}Tc-dimercaptosuccinic acid scans showed a close correlation. CeVUS can help avoid radiation exposure.

Received: July 1, 2021
Revised: December 20, 2021
Accepted: December 22, 2021

Correspondence to:
Ji Young Ha, MD, PhD, Department of Radiology, Gyeongsang National University Changwon Hospital, 11 Samjeongja-ro, Seongsan-gu, Changwon 51472, Korea

Tel. +82-55-214-3140
Fax. +82-55-214-3134
E-mail: wonpiece@gmail.com

How to cite this article:
Oh S, Ha JY, Cho YJ. Contrast-enhanced voiding ultrasonography to detect intrarenal reflux in children: comparison with 99mTc-DMSA renal scans. Ultrasonography. 2022 Jul;41(3):502-510.

Introduction

Intrarenal reflux (IRR) is an intrarenal extension of vesicoureteral reflux (VUR) into the tubular system of the kidney [1]. The incidence of IRR is reported to range from less than 1% to 10% of all reflux cases [2,3]. IRR is fundamental to the understanding of reflux-associated pyelonephritis and subsequent parenchymal scarring, which may result in hypertension and chronic renal failure [4].

In daily routine practice in Korea, both fluoroscopic voiding cystourethrography (VCUG) and acute ^{99m}Tc-dimercaptosuccinic acid (DMSA) renal scans are performed in pediatric patients with recurrent urinary tract infections (UTIs) or pyelonephritis. Fluoroscopic VCUG is generally accepted as a diagnostic modality for VUR and IRR, which are the main risk factors for recurrent acute pyelonephritis (APN) in children. As DMSA binds to the sulfhydryl groups in proximal tubules in the renal cortex, photon defects in acute DMSA renal scans provide information about the extent of renal parenchymal inflammation, and photon defects in delayed DMSA renal scans (performed 3–6 months after acute infection) show subsequent renal scarring [5,6]. Kim et al. [2] demonstrated that IRR sites on VCUG and the sites of photon defects in acute DMSA renal scans showed a close correlation, and these sites tended to progress towards renal scarring. Although clinical management decisions are based primarily on the reflux grade, and not on the presence or absence of IRR, some authors have suggested that the presence of IRR should be considered as an active measure to decrease the chances of renal scarring [2,7].

However, both VCUG and DMSA renal scans may not be suitable for pediatric patients due to the unavoidable radiation exposure and the need for procedural sedation for DMSA renal scans. From this perspective, contrast-enhanced voiding ultrasonography (CeVUS), an ionizing radiation-free alternative to fluoroscopic VCUG, is an emerging modality for the diagnosis of VUR. In addition, some reports have suggested that CeVUS could depict IRR better than conventional VCUG [8–11]. Therefore, it was hypothesized that CeVUS, which shows high sensitivity in the diagnosis of IRR, would be closely correlated with the sites of photon defects on acute DMSA renal scans.

This study aimed to evaluate the diagnostic performance of CeVUS for detecting IRR and to assess the correlation between IRR sites detected by CeVUS and sites of photon defects in acute DMSA renal scans in pediatric patients. If CeVUS and DMSA renal scans show a close correlation in detecting IRR, it is expected that CeVUS could eventually replace acute DMSA renal scans, thereby reducing patients' radiation dose.

Materials and Methods

Compliance with Ethical Standards

This prospective study was approved by the institutional review boards of the two participating hospitals (Gyeongsang National University Changwon Hospital: GNUCH 2019-06-036-002, Korea University Anam Hospital: K 2019-1208-001). Written informed consent was obtained from all parents/legal guardians, and, when applicable, the assent of the participating children was also obtained. They were informed about the purpose of the study and the advantages and disadvantages of the method.

Patient Population

From July 2019 to February 2021, pediatric patients (<18 years old) who were referred for clinically indicated CeVUS in the two participating study hospitals were enrolled in this prospective study. The indications for CeVUS were a history of recurrent febrile UTIs or pyelonephritis, prompting an assessment for VUR. All patients underwent CeVUS and acute DMSA renal scans within 7 days. The exclusion criteria included lack of consent to CeVUS and failure to obtain suitable images from CeVUS or DMSA renal scans. The medical records of eligible patients were reviewed to collect demographic data, clinical characteristics, and treatment. Leukocyturia and hematuria were defined by microscopic urinalysis, and a number of blood cells per high-power field of over 5 was considered abnormal.

Acquisition of CeVUS

All patients underwent imaging processes, including CeVUS with a baseline grayscale ultrasonographic evaluation, conducted by one of two board-certified pediatric radiologists (J.Y.H. and S.O., both having 4 years of experience in pediatric radiology). Before the studies, sterile transurethral bladder catheterization was performed in all children, followed by complete bladder emptying. The US system consisted of EPIQ 7 (Philips Healthcare, Hamburg, Germany), LOGIQ E9, or LOGIQ E10 (GE Healthcare, Milwaukee, WI, USA), using a convex transducer (C3–9 MHz) or linear high-resolution transducers (2–9 MHz). Before contrast administration, baseline grayscale images of the bladder and kidneys were acquired. The parameters assessed by the grayscale included renal parenchymal echogenicity related to APN, pelvicalyceal wall thickening, retrovesical ureteral dilatation, and the presence and grade of hydronephrosis. The ultrasonography findings of APN included altered parenchymal echogenicity, undifferentiated corticomedullary junction, and renal enlargement. Renal parenchymal echogenicity was compared with that of the liver on grayscale images. The corticomedullary junction was subjectively evaluated, and the

corticomedullary distinction was considered poor when there was no distinction between the hypoechoic medulla and the more echogenic renal cortex. Renal size was compared with that of the contralateral kidney. The grade of hydronephrosis was reported according to the urinary tract dilatation (UTD) classification system, as follows [9]; P1, central calyceal dilatation and/or anteroposterior diameter (APD) 10–15 mm; P2, peripheral calyceal dilatation and/or APD ≥15 mm; and P3, parenchymal thinning and/or an abnormal parenchymal appearance. CeVUS was performed using a low mechanical index (0.06) imaging technique after injecting sulfur hexafluoride (SonoVue, Bracco Diagnostics Inc., Monroe Township, NJ, USA) in pulse-inversion mode. CeVUS was performed after directly injecting a mixture of 0.1 mL of SonoVue with 10 mL of saline through the urethral catheter. Additional saline was then infused into the bladder through the urethral catheter via gravity. Sequential imaging of the bladder and kidneys was performed during bladder filling and voiding. Transperineal images of the urethra were obtained during voiding. Two to three CeVUS cycles of voiding were performed to increase the reflux detection rate. All examinations were performed without sedation or antibiotic prophylaxis.

Acquisition of Acute DMSA Renal Scans

Acute DMSA scans were performed for all patients to evaluate renal damage within 7 days before and after CeVUS. DMSA scans were performed with a gamma camera (Discovery NM 630, GE Healthcare or Infinia, Siemens Orbiter, Erlangen, Germany) after the intravenous injection of 37-MBq Tc-99 DMSA with weight adjustment. Single-photon emission computed tomography was performed 4 hours after the isotope was administered with a scan time of 20 minutes. All examinations were performed without sedation, and the patient usually left the radiology suite while waiting for distribution of the isotope. Four static images obtained in the anterior, posterior, right posterior oblique, and left posterior oblique projections were used for interpretation. A positive DMSA scan was defined as the presence of decreased radioactive cortical uptake in one or both kidneys. Each nuclear medicine specialist at the two institutions gave a final confirmation of cortical photon defects. The International Scientific Committee of Radionuclides in Nephrourology consensus criteria were used to interpret the DMSA scans. If photon defects were observed on a DMSA scan, we classified the location of the photon defect as the upper pole, interpolar area, or lower pole for each refluxing renal unit. Because the spatial resolution of DMSA scans is poor, the presence of multiple photon defects in a single pole was classified as only the presence or absence of a photon defect in the pole.

Image Analysis

All datasets were anonymized and randomized. Two board-certified radiologists (J.Y.H. and S.O., both having 4 years of experience in pediatric radiology), blinded to patient information, formal reports, and DMSA scans, independently reviewed CeVUS images recorded in the picture archiving and communication system. The time interval between CeVUS and image analysis was 2 months.

The presence, side, and grade of VUR were analyzed. VUR was diagnosed if microbubbles were visualized in the ureter, renal pelvis, or calyces. VUR was graded on a 5-point scale similar to the international system of radiographic grading of VUR used in VCUG [12,13]: grade 1, reflux of microbubbles into the ureter; grade 2, reflux of microbubbles up to a non-dilated pelvicalyceal system; grade 3, reflux of microbubbles up to a mildly dilated pelvicalyceal system, with no blunting or only slight blunting of the fornices; grade 4, reflux of microbubbles up to a moderately dilated pelvicalyceal system, with complete obliteration of the sharp angle of the fornices but maintenance of the papillary impressions in the majority of calyces; grade 5, reflux of microbubbles up to a severely dilated pelvicalyceal system with loss of papillary impressions and tortuous ureter.

The presence, side, type, and location of IRR were analyzed. At the height of the reflux, the renal parenchyma, showing low echogenicity, demonstrated marked hyperechogenicity, indicating IRR. The location of the IRR was classified as the upper pole, interpolar area, or lower pole for each refluxing renal unit. Likewise, in the analysis of DMSA scans, multiple IRRs in a single pole were evaluated as a single lesion, and the largest IRR was selected among multiple lesions. We classified IRR into three types according to its extent, as follows [10]: type 1 IRR, mild IRR (confined to a single medullary pyramid, which was seen as a string of tiny bubbles refluxed into the medulla with CeVUS); type 2 IRR, moderate IRR (involving several tiny bubbles refluxed into less than half of the renal parenchyma); type 3 IRR, extensive IRR (involving more than half of the renal parenchyma) (Fig. 1).

To resolve disagreements between the two reviewers regarding the absence or presence of IRR on CeVUS, another pediatric radiologist (Y.J.C. with 4 years of experience in pediatric radiology), who did not participate in the image analysis, independently reviewed discordant cases. Thereafter, the three reviewers held discussions and reached a consensus.

Statistical Analysis

Statistical analysis was performed using SPSS version 24.0 (IBM Corp., Armonk, NY, USA). For detecting IRR on CeVUS compared with photon defects on acute DMSA renal scans, sensitivity, specificity, positive predictive value, negative predictive value, and

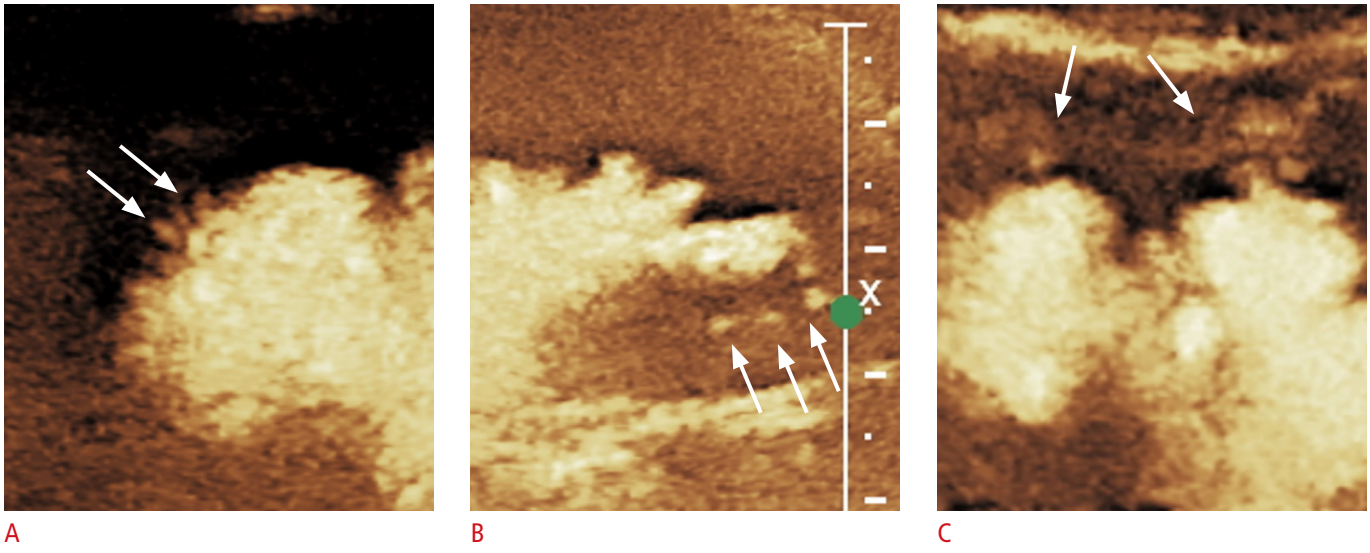

A B C D

Fig. 1. Three types of intrarenal reflux (IRR).
Three types are as follows: type 1, mild IRR: a string of tiny bubbles (arrows) refluxed into the medulla, confined to a single medullary pyramid (A); type 2, moderate IRR: several tiny bubbles (arrows) refluxed into less than half of the renal parenchyma (B, C); type 3, extensive IRR (arrows) involving more than half of the renal parenchyma (D).

accuracy were calculated. The interobserver variability regarding the types of IRR was categorized as follows: 0.81–0.99, almost perfect agreement; 0.61–0.80, substantial agreement; 0.41–0.60, moderate agreement; 0.21–0.40, fair agreement; 0.01–0.20, slight agreement, and <0.01, poor or less than chance agreement [14]. Statistical significance was set at $P<0.05$.

Results

Clinical Characteristics

The demographic characteristics of the patients are summarized in Table 1. A total of 27 patients (20 males and seven females; mean age, 5.6±4.1 months; age range, 0 to 17 months) were included from the two hospitals; three patients were enrolled at Korea University Anam Hospital and 24 patients at Gyeongsang National University Changwon Hospital, respectively. All examinations were successfully performed, and all 27 patients were included in this study without exclusion. In total, 54 renal units were evaluated, and the mean interval between CeVUS and the DMSA scan was 3.0±2.3 days.

All patients were clinically diagnosed with UTIs and leukocyturia was confirmed by urinalysis. There were 22 patients (81.5%) with positive urine cultures: *Escherichia coli* (n=15), coagulase-negative *Staphylococcus* (n=1), *Enterococcus faecium* (n=3), *Klebsiella pneumoniae* (n=2), and *Enterobacter aerogenes* (n=1).

The baseline grayscale ultrasonographic features are summarized in Table 2. Among the 54 renal units included, five renal units (9.3%) demonstrated abnormal ultrasound features suggesting APN. Twenty-one renal units (38.9%) showed pelvicalyceal wall thickening. None of the renal units showed chronic changes such as

Table 1. Patients' demographic characteristics

Characteristic	Value (n=27)
Age (year)	5.6±4.1 (0–17)
Sex (male:female)	20:7
Underlying disease	
Unilateral renal hypoplasia	1 (3.7)
Congenital hydronephrosis	3 (11.1)
UPJO, partial	1 (3.7)
Congenital adrenal neuroblastoma	1 (3.7)
Symptom	
Fever	27 (100)
Nausea/vomiting	2 (7.4)
Urine analysis	
Leukocyturia	27 (100)
Hematuria	19 (70.4)
Treatment	
Medical treatment	23 (85.2)
Surgery	4 (14.8)

Values are presented as mean±SD (range) or number (%).
UPJO, ureteropelvic junction obstruction.

Table 2. Baseline grayscale ultrasonographic features

Baseline ultrasonographic feature	Renal unit (n=54)
Presence of hydronephrosis	23/54 (42.6)
Grade of hydronephrosis[a]	
UTD-P1	14/23 (60.9)
UTD-P2	5/23 (21.7)
UTD-P3	4/23 (17.4)
Suggestive findings of APN[b]	5/54 (9.3)
Dilatation of retrovesical ureter	4/54 (7.4)
Pelvicalyceal wall thickening	21/54 (38.9)

Values are presented as number (%).
UTD, urinary tract dilatation; P, postnatal; APN, acute pyelonephritis.
[a]UTD classification; P1, central calyceal dilatation and/or anteroposterior diameter (APD) 10–15 mm; P2, peripheral calyceal dilatation and/or APD ≥15 mm; and P3, parenchymal thinning and/or abnormal parenchymal appearance. [b]Abnormal ultrasound features indicative of APN; altered parenchymal echogenicity, undifferentiated corticomedullary junction, and renal enlargement.

renal dysplasia or an irregular renal contour, which may be caused by VUR *in utero*. Hydronephrosis was detected in 23 renal units (42.6%), and the grade of hydronephrosis was as follows: UTD-P1 (n=14), UTD-P2 (n=5), and UTD-P3 (n=4). Retrovesical ureteral dilatation was detected in four renal units (7.4%).

Among the 27 patients, four underwent surgical treatment for VUR. In addition, 23 patients received medical treatment with antibiotics for the control of UTI or APN.

VUR on CeVUS

Thirteen renal units (13/54, 24.1%) of 10 patients (nine males and one female; mean age, 6.3±3.7 months; age range, 0 to 13 months) showed VUR (seven left and six right kidneys) on CeVUS. The distribution of VUR grades was as follows: grade 1, n=1; grade 2, n=1; grade 3, n=5; grade 4, n=5; grade 5, n=1. Five of 13 renal units with VUR (5/13, 38.5%) showed passive VUR before urination.

Eight renal units (8/54, 14.8%; five left and three right kidneys) in seven patients (six males and one female; mean age, 7.6±1.4 months; age range, 4 to 13 months) demonstrated IRR on CeVUS. The remaining 46 renal units (46/54, 85.2%) were negative for IRR on CeVUS. All eight renal units with IRR showed high-grade VUR (grade 3 to 5) on CeVUS (Table 3). Fifteen lesions showed IRR on CeVUS and the location of IRR were as follows: upper pole (n=8), interpolar area (n=3), and lower pole (n=4). The distribution of each IRR type was as follows: type 1 (reader 1/reader 2, n=1/n=2), type 2 (n=4/n=3), and type 3 (n=10/n=10). Interobserver agreement for the type of IRR showed almost perfect agreement, with a kappa value of 0.87 (P<0.001).

Photon Defects on Acute DMSA Renal Scan

Ten renal units (10/54, 18.5%; five left and five right kidneys) in eight patients (six males and two females; mean age, 6.9±1.4 months; age range, 2 to 13 months) showed photon defects on acute DMSA renal scans. The remaining 44 renal units (44/54, 81.5%) were negative on acute DMSA renal scans. A total of 19 lesions in 10 renal units showed photon defects on acute DMSA scans, and four renal units showed multifocality. The location of the photon defects was as follows: upper pole (n=8), interpolar area (n=7), and lower pole (n=4).

Comparison between CeVUS and Acute DMSA Renal Scans

In a comparison between the findings of IRR on CeVUS and photon defects on acute DMSA, 52 renal units (96.3%) showed concordant results, and two renal units (3.7%) showed discordant results. In the per-renal-unit analysis, the sensitivity, specificity, positive predictive value, negative predictive value, and accuracy of IRR detection on CeVUS were 80%, 100%, 100%, 95.7%, and 96.3%, respectively.

In the per-lesion analysis, 15 photon defects on acute DMSA (15/19, 78.9%) showed IRR on CeVUS (Fig. 2). Four lesions showed discordant results, and all discordant lesions were located in the interpolar area. All lesions of IRR on CeVUS showed photon defects on DMSA renal scans, regardless of the type of IRR.

Discussion

We compared the results of CeVUS to those of acute DMSA scans

Table 3. DMSA scan and CeVUS findings in eight patients with photon defects

Patient No.	Renal unit	Right/Left	Location	Photon defect	IRR	Concordance	VUR grade
5	1	Left	Upper pole	+	+	Concordant	4
			Interpolar area	+	+	Concordant	
7	2	Right	Upper pole	+	+	Concordant	4
			Interpolar area	+	+	Concordant	
			Lower pole	+	+	Concordant	
8	3	Right	Interpolar area	+	–	Discordant	2
10	4	Right	Upper pole	+	+	Concordant	4
			Interpolar area	+	–	Discordant	
			Lower pole	+	+	Concordant	
	5	Left	Upper pole	+	+	Concordant	3
			Interpolar area	+	–	Discordant	
			Lower pole	+	+	Concordant	
16	6	Right	Interpolar area	+	–	Discordant	3
	7	Left	Upper pole	+	+	Concordant	4
			Interpolar area	+	+	Concordant	
			Lower pole	+	+	Concordant	
17	8	Left	Upper pole	+	+	Concordant	4
19	9	Left	Upper pole	+	+	Concordant	5
23	10	Right	Upper pole	+	+	Concordant	3

DMSA, ^{99m}Tc-dimercaptosuccinic acid renal scan; CeVUS, contrast-enhanced voiding ultrasonography; IRR, intrarenal reflux; VUR, vesicoureteral reflux.

to evaluate the diagnostic performance of CeVUS for detecting IRR and evaluated the substitutability of CeVUS for acute DMSA scans. In this study, CeVUS and acute DMSA renal scans showed a close correlation (96.3%) in detecting IRR. In the per-renal-unit analysis, CeVUS showed excellent sensitivity (80%) and negative predictive value (95.7%), as well as perfect specificity (100%) and positive predictive value (100%). Furthermore, in the per-lesion analysis, 19 lesions in 10 kidneys showed photon defects on acute DMSA scans and 15 lesions (15/19, 78.9%) correlated with IRR in CeVUS with high interobserver agreement.

IRR involves the reflux of urine from the calyceal system into the collecting tubules, which occurs in association with compound renal papillae at the polar regions of the kidneys, and acts as a marker of potential sites of renal parenchymal scarring [15,16]. Simicic Majce et al. [11] reported that the patients with IRR-associated VUR showed an earlier clinical presentation. The management of reflux with IRR remains controversial. Kim et al. [2] and Fukui et al. [17] suggested that VUR with IRR should be treated more aggressively to decrease the risk of renal scarring. Kim et al. [2] reported that for VUR with IRR, patients undergoing surgical treatment showed a lower rate of renal scarring detected by follow-up DMSA scans every 3–6 months than patients receiving prophylactic antibiotics. Fukui et al. [17] reported that patients with IRR were more likely to present with decreased differential renal function in DMSA scans and breakthrough UTIs; therefore, surgical treatment should be considered more frequently in cases with IRR. Meanwhile, Boubnova et al. [7] reported that high-grade reflux with IRR showed no statistically significant difference from high-grade reflux without IRR in terms of the frequency of UTIs, the stability of renal status on DMSA scans, and spontaneous resolution after medical treatment during 3 years of follow-up. However, an animal model of VUR in piglets showed that the combination of VUR, IRR, and urinary infection is a necessary precondition for parenchymal scarring to develop [18]. Therefore, IRR of infected urine is believed to play a role in the pathogenesis of reflux-associated pyelonephritis and subsequent parenchymal scarring, and the detection of IRR may play an important role in determining the treatment plan.

Recently, the Food and Drug Administration (December 2016) and the European Medicines Agency (June 2017) approved an ultrasonography contrast agent, sulfur hexafluoride lipid-type A microspheres, for studying the pediatric urinary tract to detect VUR in the United States and Europe [19,20]. The application of ultrasonography contrast agents has enabled CeVUS to provide functional information on reflux in addition to detailed anatomical information about the urinary system without any radiation risk [13]. The pediatric radiation dose should be very carefully monitored and

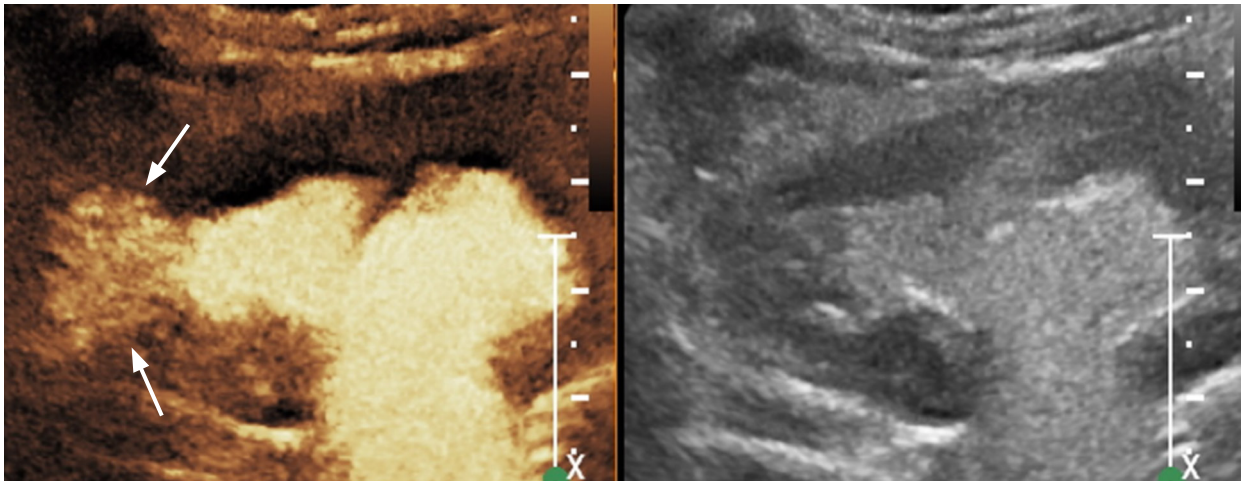

A

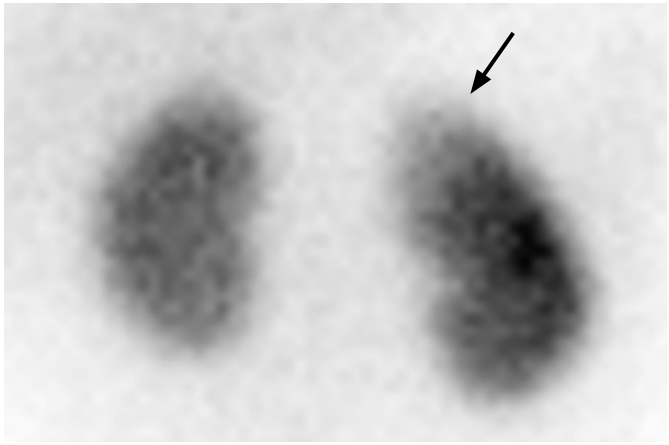

B

Fig. 2. A 5-month-old infant after a urinary tract infection with left grade 4 vesicoureteral reflux (patient 17 in Table 3).
Dual-screen contrast-enhanced ultrasound image of the left kidney is shown. A. Type 3 extensive intrarenal reflux (arrows) was detected in the upper pole of the left kidney. B. A ^{99m}Tc-dimercaptosuccinic acid renal scan shows a photon defect (arrow) in the corresponding area with contrast-enhanced voiding ultrasonography.

optimized considering the increased risk of complications in infants and children, and pediatric patients indicated for fluoroscopic VCUG are most vulnerable to radiation. In addition to CeVUS being free of ionizing radiation, recent case series and studies have shown that CeVUS may be comparable to or better than VCUG for IRR detection [8,10]. Kim et al. [10] reported that IRR was more frequently detected with CeVUS than with VCUG, while three cases (30%, 3/10) of IRR were detected using VCUG, and 10 cases (100%, 10/10) were detected using CeVUS. Simicic Majce et al. [11] also reported that the incidence of IRR increased according to the severity of VUR by utilizing CeVUS, which has a high ability to detect IRR. The present study showed that IRR detected on CeVUS was correlated with photon defects on acute DMSA scans. To the best of our knowledge, this study is the first to evaluate the performance of CeVUS compared with photon defects on acute DMSA scans in detecting IRR. Our results suggest the possibility that CeVUS might replace acute DMSA renal scans, thereby reducing the radiation dose in pediatric patients. Furthermore, IRR detected using CeVUS can be targeted for appropriate therapeutic management, including surgery, to prevent disease progression (renal scarring).

In the present study, the authors' centers did not use sedatives for the DMSA renal scan. However, some centers routinely use sedation in pediatric patients. For DMSA renal scans in infants and young children, procedural sedation to minimize the child's discomfort might be necessary [21]. It is also known that the radiation dose of ^{99m}Tc-DMSA renal scans for infants and children is very low (<0.7 mSv) [22]. Therefore, physicians do not pay close attention to radiation exposure in DMSA renal scans. However, reducing the radiation dose, even by small amounts, remains an important issue, especially in young patients who are particularly susceptible to the adverse effects of ionizing radiation. If CeVUS replaces acute DMSA renal scans, as our study suggests might be possible, it would have the advantages of lowering sedative use and radiation hazards.

A recent study showed close correlations of cortical perfusion

defects on contrast-enhanced ultrasonography (CEUS), implying APN, with photon defects on DMSA renal scans and computed tomography (80.3% and 84.6%, respectively) in pediatric patients [23]. In contrast, the present study compared IRR on CeVUS with photon defects on acute DMSA renal scans. As DMSA binds to the sulfhydryl groups in proximal tubules in the renal cortex, photon defects in acute DMSA renal scans demonstrate the extent of renal parenchymal inflammation, which is thought to be consistent with the region of perfusion defect in CEUS, while not exactly representing IRR. However, according to a previous study [2], IRR sites on VCUG and the sites of photon defects in acute DMSA renal scans show a close correlation, and these sites tended to progress towards renal scarring. The findings of this study allow the inference that lesions with IRR are associated with renal parenchymal inflammation, and could have a high tendency for renal scarring, which is clinically significant.

This study has certain limitations that should be considered when interpreting the findings. First, there was an unavoidable selection bias due to the small study population enrolled with a small number of IRR cases. To overcome this limitation, this study was conducted at two centers; however, the sample size was still small. A large-scale investigation may be necessary to determine the clinical significance of IRR detected using CeVUS compared with acute DMSA renal scans. Second, DMSA scans and CeVUS studies were not conducted on the same day. The mean interval between the two studies was as short as 3.0±2.3 days; however, the patients were already being treated with antibiotics during hospitalization. Third, we analyzed the locations of photon defects on DMSA scans and CeVUS. Due to the poor spatial resolution, we cannot be sure whether the two studies displayed defects of the same lesion in the same location. Therefore, we only acknowledged the presence or absence of photon defects in each pole when there were multiple photon defects in a single pole. Fourth, in the per-lesion analysis, all discordant lesions (4/19 lesions) between photon defects and IRR were all in the interpolar area of the kidney (Table 3). The cause of this result might have been that in the present study, the renal scans in the CeVUS procedures were mainly performed with the longitudinal scan plane, parallel to the long diameter of the kidney, to evaluate the entire kidney in a short time. Although the longitudinal scan plane is easier for differentiating the anatomical relationships of the kidney, such as the pelvicalyceal system and location, using the transverse scan plane is necessary to evaluate the relatively thick renal parenchyma of the interpolar area. Even though we tried to scan both planes during CeVUS procedure, more careful scanning of the transverse scan plane in CeVUS procedure might help reduce the possibility of missing the interpolar area. Finally, in the per-lesion analysis, four lesions showed a discrepancy between IRR detected using CeVUS and photon defects on acute DMSA renal scans. The discrepancies between IRR detected using CeVUS and photon defects on acute DMSA renal scans may be a prognostic factor for disease progression towards renal scarring. Further prospective studies are required to evaluate the long-term outcomes.

In conclusion, this study showed that CeVUS had good performance in detecting IRR, and the IRR sites detected by CeVUS were closely correlated with photon defect sites in acute DMSA scans. These findings suggest that CeVUS may play an important role in managing patients with recurrent UTIs or pyelonephritis with reduced radiation exposure.

ORCID: Saelin Oh: https://orcid.org/0000-0002-3815-5599; Ji Young Ha: https://orcid.org/0000-0001-5769-3045; Yeon Jin Cho: https://orcid.org/0000-0001-9820-3030

Author Contributions

Conceptualization: Ha JY. Data acquisition: Oh S, Ha JY. Data analysis or interpretation: Ha JY, Cho YJ. Drafting of the manuscript: Oh S, Ha JY. Critical revision of the manuscript: Oh S, Ha JY, Cho YJ. Approval of the final version of the manuscript: all authors.

Conflict of Interest

This work was supported by a grant from Bracco imaging Korea, Ltd. (Seoul, South Korea). All remaining authors have no conflicts of interest.

References

1. Gotoh T, Asano Y, Nonomura K, Togashi M, Koyanagi T. Intrarenal reflux in children with vesicoureteral reflux. Nihon Hinyokika Gakkai Zasshi 1991;82:1480-1486.
2. Kim SW, Im YJ, Hong CH, Han SW. The clinical significance of intrarenal reflux in voiding cystourethrography (VCUG). Korean J Urol 2010;51:60-63.
3. Schneider KO, Lindemeyer K, Kammer B. Intrarenal reflux, an overlooked entity: retrospective analysis of 1,166 voiding cysturethrographies in children. Pediatr Radiol 2019;49:617-625.
4. Geback C, Hansson S, Martinell J, Sandberg T, Sixt R, Jodal U. Renal function in adult women with urinary tract infection in childhood. Pediatr Nephrol 2015;30:1493-1499.
5. Muller-Suur R, Gutsche HU. Tubular reabsorption of technetium-99m-DMSA. J Nucl Med 1995;36:1654-1658.
6. Shukla J, Mittal BR. Dimercaptosuccinic acid: a multifunctional cost effective agent for imaging and therapy. Indian J Nucl Med 2015;30:295-302.
7. Boubnova J, Sergent-Alaoui A, Deschenes G, Audry G. Evolution

and prognosis value of intrarenal reflux. J Pediatr Urol 2011;7:638-643.
8. Colleran GC, Barnewolt CE, Chow JS, Paltiel HJ. Intrarenal reflux: diagnosis at contrast-enhanced voiding urosonography. J Ultrasound Med 2016;35:1811-1819.
9. Darge K, Trusen A, Gordjani N, Riedmiller H. Intrarenal reflux: diagnosis with contrast-enhanced harmonic US. Pediatr Radiol 2003;33:729-731.
10. Kim D, Choi YH, Choi G, Lee S, Lee S, Cho YJ, et al. Contrast-enhanced voiding urosonography for the diagnosis of vesicoureteral reflux and intrarenal reflux: a comparison of diagnostic performance with fluoroscopic voiding cystourethrography. Ultrasonography 2021;40:530-537.
11. Simicic Majce A, Arapovic A, Saraga-Babic M, Vukojevic K, Benzon B, Punda A, et al. Intrarenal reflux in the light of contrast-enhanced voiding urosonography. Front Pediatr 2021;9:642077.
12. Darge K, Troeger J. Vesicoureteral reflux grading in contrast-enhanced voiding urosonography. Eur J Radiol 2002;43:122-128.
13. Duran C, Beltran VP, Gonzalez A, Gomez C, Riego JD. Contrast-enhanced voiding urosonography for vesicoureteral reflux diagnosis in children. Radiographics 2017;37:1854-1869.
14. Landis JR, Koch GG. The measurement of observer agreement for categorical data. Biometrics 1977;33:159-174.
15. Ransley PG. Intrarenal reflux: anatomical, dynamic and radiological studies-part I. Urol Res 1977;5:61-69.
16. Rose JS, Glassberg KI, Waterhouse K. Intrarenal reflux and its relationship to renal scarring. J Urol 1975;113:400-403.
17. Fukui S, Watanabe M, Yoshino K. Intrarenal reflux in primary vesicoureteral reflux. Int J Urol 2013;20:631-636.
18. Arnold AJ, Sunderland D, Hart CA, Rickwood AM. Reconsideration of the roles of urinary infection and vesicoureteric reflux in the pathogenesis of renal scarring. Br J Urol 1993;72:554-556.
19. U.S. Food and Drug Administration. Drugs@FDA: FDA-approved drugs-Lumason [Internet]. Silver Spring, MD: U.S. Food & Drug Administration, 2014 [cited 2021 Jun 8]. Available from: https://www.accessdata.fda.gov/scripts/cder/daf/index.cfm?event=overview.process&applno=203684.
20. European Medicines Agency, Committee for Medicinal Products for Human Use. SonoVue [Internet]. London: European Medicines Agency, 2017 [cited 2021 Jun 8]. Available from: https://www.ema.europa.eu/en/documents/smop/chmp-post-authorisation-summary-positive-opinion-sonovue_en.pdf.
21. Shaikh N, Hoberman A, Keren R, Ivanova A, Ziessman HA, Cui G, et al. Utility of sedation for young children undergoing dimercaptosuccinic acid renal scans. Pediatr Radiol 2016;46:1573-1578.
22. O'Reilly SE, Plyku D, Sgouros G, Fahey FH, Ted Treves S, Frey EC, et al. A risk index for pediatric patients undergoing diagnostic imaging with (99m)Tc-dimercaptosuccinic acid that accounts for body habitus. Phys Med Biol 2016;61:2319-2332.
23. Jung HJ, Choi MH, Pai KS, Kim HG. Diagnostic performance of contrast-enhanced ultrasound for acute pyelonephritis in children. Sci Rep 2020;10:10715.